THE JOURNAL OF BIOLOGICAL CHEMISTRY
Vol. 279, No. 23, Issue of June 4, pp. 24179–24188, 2004
Printed in U.S.A.

Selective Roles for Tumor Necrosis Factor α-converting Enzyme/ADAM17 in the Shedding of the Epidermal Growth Factor Receptor Ligand Family

THE JUXTAMEMBRANE STALK DETERMINES CLEAVAGE EFFICIENCY*

Received for publication, November 5, 2003, and in revised form, March 31, 2004
Published, JBC Papers in Press, April 5, 2004, DOI 10.1074/jbc.M312141200

C. Leann Hinkle‡, Susan W. Sunnarborg‡, David Loiselle§, Carol E. Parker§, Mary Stevenson¶, William E. Russell¶, and David C. Lee‡‖**

From the ‡Department of Biochemistry and Biophysics, §University of North Carolina Proteomics and Mass Spectrometry Facility and ‖Lineberger Comprehensive Cancer Center, University of North Carolina School of Medicine, Chapel Hill, North Carolina 27599 and the ¶Departments of Pediatrics and Cell Biology, Vanderbilt University, Nashville, Tennessee 37232

Epidermal growth factor (EGF) family ligands are derived by proteolytic cleavage of the ectodomains of integral membrane precursors. Previously, we established that tumor necrosis factor α-converting enzyme (TACE/ADAM17) is a physiologic transforming growth factor-α (TGF-α) sheddase, and we also demonstrated enhanced shedding of amphiregulin (AR) and heparin-binding (HB)-EGF upon restoration of TACE activity in TACE-deficient EC-2 fibroblasts. Here we extended these results by showing that purified soluble TACE cleaved single sites in the juxtamembrane stalks of mouse pro-HB-EGF and pro-AR ectodomains *in vitro*. For pro-HB-EGF, this site matched the C terminus of the purified human growth factor, and we speculate that the AR cleavage site is also physiologically relevant. In contrast, ADAM9 and -10, both implicated in HB-EGF shedding, failed to cleave the ectodomain or cleaved at a nonphysiologic site, respectively. Cotransfection of TACE in EC-2 cells enhanced phorbol myristate acetate-induced but not constitutive shedding of epiregulin and had no effect on betacellulin (BTC) processing. Additionally, soluble TACE did not cleave the juxtamembrane stalks of either pro-BTC or pro-epiregulin ectodomains *in vitro*. Substitution of the shorter pro-BTC juxtamembrane stalk or truncation of the pro-TGF-α stalk to match the pro-BTC length reduced TGF-α shedding from transfected cells to background levels, whereas substitution of the pro-BTC P2-P2′ sequence reduced TGF-α shedding less dramatically. Conversely, substitution of the pro-TGF-α stalk or lengthening of the pro-BTC stalk, especially when combined with substitution of the pro-TGF-α P2–P2′ sequence, markedly increased BTC shedding. These results indicate that efficient TACE cleavage is determined by a combination of stalk length and scissile bond sequence.

The epidermal growth factor (EGF)[1] family includes seven structurally related proteins as follows: EGF, transforming growth factor-α (TGF-α), amphiregulin (AR), heparin-binding epidermal growth factor (HB-EGF), betacellulin (BTC), epiregulin (EPR), and epigen (reviewed in Ref. 1). Members of this family share a distinctive disulfide-bonded 3-loop domain, the EGF-like motif, which is required for high affinity binding to the EGF receptor (EGFR). Soluble receptor ligands containing this EGF-like sequence are in each case released from integral membrane precursor proteins. The critical "C-terminal" cleavage events that are required for release occur within short juxtamembrane stalks that link the EGF-like motifs to the transmembrane (TM) domains. Additionally, variable cleavage at membrane distal sites (N-terminal cleavage) gives rise to larger soluble forms and could modulate the function of EGF family members. Whether both C- and N-terminal processing events are mediated by the same or different enzymes is presently unclear.

Although both integral membrane and soluble growth factors have been shown to activate EGFR (2–5) with potentially different consequences (6–9), the observed phenotypes of EGF family knockouts are consistent with paracrine roles for these growth factors (10–14), and some biological responses may be impaired by preventing release of soluble growth factor (7, 15–18). Moreover, regulated shedding of EGF ligands has been linked recently to G-protein-coupled receptor-mediated EGFR transactivation (1, 19–24). Thus, identifying the mechanisms that govern EGF family shedding is critical to an understanding of the regulation of EGF family/EGFR action.

Several lines of evidence have implicated the disintegrin and metalloprotease TACE/ADAM17 (25, 26) in the release of soluble TGF-α, a well studied model of ectodomain shedding. Mice homozygous for a mutant TACE gene ($TACE^{\Delta Zn}$) encoding an inactive enzyme displayed the same open eye at birth and wavy

* This work was supported by National Institutes of Health Training Grant CA71341 (to C. L. H.) and Grants CA85410 (to D. C. L.) and DK53804 (to W. E. R.). The costs of publication of this article were defrayed in part by the payment of page charges. This article must therefore be hereby marked "*advertisement*" in accordance with 18 U.S.C. Section 1734 solely to indicate this fact.

** To whom correspondence should be addressed: Dept. of Biochemistry and Biophysics, CB 7260, University of North Carolina School of Medicine, Chapel Hill, NC 27599-7260. Tel.: 919-966-5912; Fax: 919-966-2852; E-mail: dclee@med.unc.edu.

[1] The abbreviations used are: EGF, epidermal growth factor; TGF-α, transforming growth factor α; AR, amphiregulin; HB-EGF, heparin-binding epidermal growth factor; BTC, betacellulin; EPR, epiregulin; EGFR, epidermal growth factor receptor; TNFα, tumor necrosis factor α; TACE, tumor necrosis factor α-converting enzyme; ADAM, a disintegrin and metalloprotease; JM, juxtamembrane domain; TM, transmembrane domain; FBS, fetal bovine serum; PBS, phosphate-buffered saline; PMA, phorbol myristate acetate; HA, hemagglutinin; ELISA, enzyme-linked immunosorbent assay; MALDI/TOF-MS, matrix-assisted laser desorption/ionization time-of-flight mass spectrometry; MMP, matrix metalloprotease; DMEM, Dulbecco's modified Eagle's medium; CHO, Chinese hamster ovary; TPA, 12-*O*-tetradecanoylphorbol-13-acetate; GPCR, G-protein-coupled receptors; Pan, pantothenate.

whisker (27) phenotype as TGF-α- (10, 11) and EGFR-null (28–30) mice. Fibroblasts, as well as primary keratinocytes, derived from these TACE-deficient mice, were dramatically impaired in their ability to shed TGF-α, whereas restoration of functional TACE enhanced processing (27, 31). Moreover, soluble TACE correctly cleaved the pro-TGF-α ectodomain at both N- and C-terminal processing sites *in vitro* (31). Collectively, these results established TACE as a major TGF-α sheddase, although TACE-deficient cells retain reduced ability to shed TGF-α, apparently because of the minor action of one or more other metalloproteases (32, 33).

TACE-deficient mice die soon after birth, displaying epithelial defects in lung, small intestine, stomach, thyroid, parathyroid, and salivary glands (27). These defects are broadly similar to those observed in EGFR null mice, prompting speculation that TACE is a Pan-EGF family sheddase (27, 34). Supporting this notion, TACE-deficient and HB-EGF-null mice displayed similarly defective cardiac valvulogenesis and poorly differentiated lungs (14, 35), and cotransfection of TACE with pro-AR and pro-HB-EGF increased the shedding of these growth factors from TACE-deficient fibroblasts (31). In addition, application of TACE antisense oligonucleotides or small interfering RNA diminished AR shedding from lung (36) and HNSCC cells (24). Arguing against a role for TACE as a Pan-EGF family convertase, EGF processing was shown to be metalloprotease-dependent, but TACE-independent (37), and ADAM9 (38), -10 (23, 39), and -12 (21, 40) have all been implicated in HB-EGF shedding in cell and animal models.

Here we used cell-based and *in vitro* assays to examine further the role of TACE as a mediator of EGF family shedding. Our results support recent genetic evidence implicating TACE as a physiologic HB-EGF convertase, while arguing against roles for ADAM9 and -10, and they are also consistent with growing evidence that TACE is a major AR convertase. On the other hand, although TACE contributed to PMA-induced shedding of EPR, it did not affect constitutive release of either EPR or BTC, nor did it efficiently cleave the ectodomains of pro-BTC or pro-EPR *in vitro*. Through stalk domain swapping and mutagenesis experiments aimed at understanding TACE preference for pro-TGF-α *versus* pro-BTC, we found that in addition to scissile bond sequence, stalk length is a major determinant of which EGF family precursors are efficient TACE substrates.

EXPERIMENTAL PROCEDURES

Materials—The antibodies used are as follows: monoclonal anti-HA.11 (Covance Research Products, Denver, PA), monoclonal anti-FLAG M2 (Sigma), polyclonal anti-human TGF-α (Sigma), and polyclonal anti-mouse BTC (R & D Systems, Minneapolis, MN). Peroxidase-conjugated secondary antibodies were from Roche Applied Science or Santa Cruz Biotechnology. The M2 monoclonal anti-FLAG affinity gel was obtained from Sigma, and the anti-HA affinity resin and peptide were from Roche Applied Science. Oligonucleotide primers were synthesized by the University of North Carolina Lineberger Comprehensive Cancer Center Nucleic Acids Core Facility. The QuickChange Site-directed Mutagenesis kit (Stratagene, La Jolla, CA) was used to insert HA and FLAG epitopes and to construct EGF family ectodomains and juxtamembrane domain mutants per the manufacturer's instructions.

Construction of Epitope-tagged Growth Factors—Murine cDNAs for the murine EGF ligands were epitope-tagged with HA and FLAG sequences (31, 41). Forward primers used for mutagenesis are as follows: AR FLAG, 5′-GGGACTGTGCACGCCGATTACAAGGACGACGATGACAAGATTGCCTAG-3′; HB-EGF FLAG, 5′-GGGCGTGGCTAGCGATTACAAGGACGACGATGACAAGTCCCACTGAGG-3′; BTC HA, 5′-CCTAGACAGAAAGTGAAAACCCACTACCCATACGACGTCCCAGACTACGCTTTCTCTCGGTGCCCC-3′; BTC FLAG, 5′-CCATAAGTGAAGATATTCAAGAGACCAATGATTACAAGGACGACGATGACAAGATTGCTTAACGG-3′; EPR HA,: 5′-GGCTCAAGTGCAGATTTACCCATACGACGTCCCAGACTACGCTACAAAGTGTAGTTCTGACATGG-3′; and EPR FLAG, 5′-GGACCCAGTGCTGCCAGATTACAAGGACGACGATGACAAGCAGGTCTGAAAGC-3′. All cDNAs were expressed in pcDNA3 (Invitrogen), except pro-EPR, which was cloned into pSI (Promega Corp., Madison, WI) for optimal expression (42).

Transfection and Western Blot Analysis—EC-2 fibroblasts (43) were grown in Dulbecco's modified Eagle's medium-F12 (DMEM/F-12) with 1% fetal bovine serum (FBS) and transfected in serum-free media with the indicated cDNAs by using LipofectAMINE (Invitrogen). Chinese hamster ovary (CHO) cells were grown in DMEM with 5% FBS and 1× nonessential amino acids and transfected by using FuGENE 6 (Roche Applied Science). For TAPI-2 experiments, cells were switched to complete media in the presence or absence of 50 μM TAPI-2 (Peptides International, Louisville, KY) after 24 h. After 24 h, conditioned media and cell lysates were harvested. For PMA experiments, cells were switched to complete media after 24 h. After 24 h, cells were washed with serum-free media and incubated in serum-free media in the presence and absence of 100 ng/ml PMA (Sigma) for 2 h (43) before conditioned media and cell lysates were harvested. For each PMA experiment sample, media or lysate from three transfected 60-mm dishes were pooled and treated together. All media was concentrated on Sep-Pak C-18 cartridges (Waters) and lyophilized (44). To collect lysates, cells were washed in 1× phosphate-buffered saline (PBS) and lysed in 50 mM Tris, pH 7.4, 150 mM NaCl, 1% Triton X-100 with protease inhibitors (10 μg/ml leupeptin, 20 μg/ml aprotinin, 1 mM phenylmethylsulfonyl fluoride (PMSF), and 1 μM EDTA). Protein concentrations were determined by using the BCA Protein Assay (Pierce). Conditioned media and cell lysates (75 μg) were analyzed by Western blot (31) as indicated.

Sandwich ELISA—To quantitate nanogram levels of epitope-tagged growth factors, we developed a sandwich ELISA for TGF-α and BTC similarly to published protocols (45). Briefly, 96-well enzyme immunoassay/radioimmunoassay high binding plates (Corning Glass) were incubated with 10–15 μg/ml anti-HA overnight at room temperature. After each incubation, wells were washed three times with wash buffer (1× PBS, 0.05% Tween 20). Wells were blocked in 2% BSA, 1× PBS, 0.05% Tween 20 for 1 h at room temperature. Media and lysate samples or standards (ligand ectodomains) were diluted in dilution buffer (2% FBS, 1× PBS, 0.05% Tween 20), added to wells in triplicate, and incubated for 1.5 h at room temperature. Anti-growth factor antibodies diluted 1:100 (anti-TGF-α) or 1:200 (anti-BTC) in dilution buffer were added for 1.5 h at room temperature. Anti-goat horseradish peroxidase (Santa Cruz Biotechnology) diluted 1:10,000 in dilution buffer was added for 1 h at room temperature. Color substrate solution (R & D Systems, Minneapolis, MN) was added to wells and incubated for 20 min at room temperature in the dark. The color reaction was stopped by adding 1.5 N sulfuric acid and immediately read on a plate reader at 450 nm.

Production of Ectodomain Ligands—Pro-TGF-ecto was generated previously (31). Forward primers used for mutagenesis are as follows: ProARecto, 5′-GCGAGGATGACAAGGACCTATCCAAGGATTACAAGGACGACGATGACAAGATTGCC-3′; ProHB-EGFecto, 5′-CCTATACACATATGACCACACTGATTACAAGGACGACG-3′; Pro-BTCecto: 5′-GCAGGACCGGGGGCAGGATTACAAGGACGACG-3′; and Pro-EPRecto, 5′-CGTTGACAGTGATTCTCATTTTCGATTACAAGGACGACG-3′.

To produce ectodomain proteins, cDNAs were transfected into COS-1 cells using FuGENE 6 (Roche Applied Science). After 24 h, cells were placed in complete media (DMEM, 10% FBS) and cultured for an additional 24 h before conditioned media were collected. For pro-BTCecto and pro-EPRecto, conditioned media were concentrated as before (31). For pro-ARecto and pro-HB-EGFecto, media were immunoprecipitated by using anti-HA affinity resin at 4 °C with tumbling for 24–48 h. Beads were washed with 20 bed volumes of wash buffer (20 mM Tris, pH 7.5, 0.1 M NaCl, 0.1 mM EDTA, 0.05% Tween 20), and bound proteins were eluted by using 1 mg of HA peptide in equilibration buffer (20 mM Tris, pH 7.5, 0.1 M NaCl, 0.1 mM EDTA) at 37 °C with tumbling. To remove excess HA peptide, proteins were dialyzed against 10 mM Tris, pH 8.0, at 4 °C for 16–18 h using Spectra-Por membrane (10,000 molecular weight cut-off) (Spectrum Laboratories Inc., Rancho Dominguez, CA). The protein concentrations were assayed using the BCA Protein Assay (Pierce) and normalized for ectodomain proteins by comparison on Western blots.

In Vitro Digests—Aliquots (1–10 μg) of ectodomain proteins were incubated with 150–300 μg/ml recombinant human TACE or ADAM9 or ADAM10 (R & D Systems) or 10 mM Tris, pH 8.0 (as indicated) (31), for 1 or 24 h. Reactions were stopped by adding SDS-PAGE sample buffer, and products were separated by SDS-PAGE, transferred to Immobilon polyvinylidene difluoride, and probed with the indicated antibodies. For determination of N- and C-terminal cleavage sites, reactions were stopped by adding 10 mM EDTA, and products were

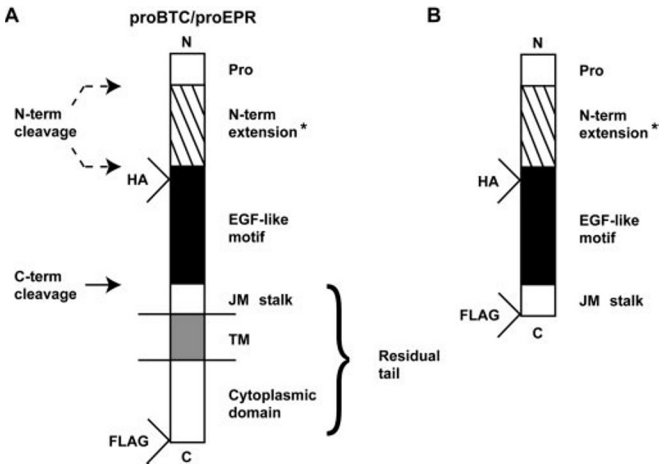

FIG. 1. **Constructs used in this study.** *A*, representative schematic of full-length epitope-tagged EGF family members (signal peptides not shown). The abbreviations used are as follows: *Pro*, prodomain; *JM*, juxtamembrane stalk. The EGF-like sequence is denoted by the *black box*. *, an N-terminal extension, indicated by the *hatched box*, is present in pro-AR, pro-BTC, and pro-HB-EGF; and N-terminal (*N-term*) cleavage occurs at various sites (*dashed arrows*). C-terminal (*C-term*) cleavage site is indicated by a *solid arrow*, and the residual tail (TM/cytoplasmic domains) is indicated by a *bracket*. The locations of the HA and FLAG tags are indicated. *B*, representative schematic of epitope-tagged ectodomain constructs. The FLAG epitope is followed in each case by the two C-terminal amino acids from the cytoplasmic domain of the precursor (31).

immunoprecipitated by using M2 anti-FLAG affinity gel at 4 °C for 16–18 h. Beads were washed five times with fresh 50 mM ammonium bicarbonate. Molecular weights of cleavage products were determined by matrix-assisted laser desorption/ionization time-of-flight mass spectrometry (MALDI/TOF-MS) using a Bruker Reflex III mass spectrometer (Bruker Instruments Co., Billerica, MA) optimized in the linear mode (46, 47), and recrystallized α-cyano-4-hydroxycinnamic acid (Aldrich) was used as the matrix. The α-cyano-4-hydroxycinnamic acid solvent was 50:50:0.1 acetonitrile/water/trifluoroacetic acid and used as a saturated solution. A 0.5-μl aliquot of the settled beads was spotted on the target, followed by 0.5 μl of matrix solution, and the solution was allowed to dry at room temperature.

Construction of Juxtamembrane Domain Mutants—Epitope-tagged pro-TGF-α (41) and pro-BTC cDNAs were used to construct juxtamembrane domain mutants. For the BTC-$JM_{FYLQ\text{-}LAVV}$+2 mutant, sequential rounds of mutagenesis were performed using the BTC-$JM_{FYLQ\text{-}LAVV}$ and BTC-JM+2 primers. Forward primers used are as follows: TGF-JMBTC, 5′-GGTGTTCGCTGTGAGCGAGTGGACCTGTTTTACCTCCAGCAGGACCGGGGGCAGGCCATCACTGCCCTGG-3′; TGF-JMΔ2, 5′-GCTGCCAGCCAGAAGGCCATCACTGCCC-3′; TGF-$JM_{LAVV\text{-}FYLQ}$, 5′-CGCTGTGAGCATGCAGACCTCTTTTACCTCCAGGCTGCCAGCCAGA AGAAGC-3′; BTC-JMTGF-, 5′-GGCTACTTTGGGGCTCGGTGTGAGCATGCAGACCTCCTGGCTGTGGTGGCTGCCAGCCAGAAGAAGCAAATCCTGGTGGTCTGCTTGATAGTGG-3′; BTC-JM+2, 5′-GCAGGACCGGGGGCAGAAGCAAATCCTGGTGGTCTGC-3′; and BTC-$JM_{FYLQ\text{-}LAVV}$, 5′-GGTGTGAGCGAGTGGACCTGCTTGCCGTCGTGCAGGACCGGGG G-3′.

Statistical Analysis—Statistical analysis was performed by the University of North Carolina Lineberger Comprehensive Cancer Center Biostatistics Facility using SAS statistical software, version 8.2 (SAS Institute Inc., Cary, NC), and the Wilcoxon rank sum test for pairwise group comparisons. *p* values are exact and have been adjusted by using the Bonferroni method to allow multiple comparisons.

RESULTS

TACE Does Not Enhance Shedding of Betacellulin or Epiregulin from Cells—We showed previously that cotransfection of TACE with TGF-α, AR, or HB-EGF enhanced shedding of these growth factors from TACE-deficient (EC-2) fibroblasts (31). To assess the role of TACE in the shedding of two additional EGF family members, BTC and EPR, we generated epitope-tagged constructs encoding the precursors (Fig. 1*A*). As with pro-TGF-α (41), the HA epitope was inserted into the N-terminal portion of the EGF-like sequence, either three (BTC) or two (EPR) amino acids upstream of the first cysteine. In both cases, the FLAG epitope was inserted into the cytoplasmic domain of the precursor immediately preceding the penultimate amino acid. Tagged pro-BTC or pro-EPR were transfected into EC-2 fibroblasts, which lack functional TACE (43), in the presence or absence of TACE cDNA, and lysates and conditioned media were analyzed by Western blot by using HA and FLAG antibodies. Pro-TGF-α and empty pcDNA3 vector were transfected as positive and negative controls.

As observed previously (31), lysates of TGF-α-transfected EC-2 cells (43) contained 36- and 20–25-kDa species that were recognized by both anti-HA (Fig. 2*A*) and anti-FLAG (data not shown); the 36-kDa form is the fully glycosylated precursor, and the 20–25-kDa forms are immature glycoprotein precursors (41). FLAG, but not HA antibody, also recognized a minor 16-kDa species corresponding to the residual transmembrane (TM)/cytoplasmic domains of pro-TGF-α (Fig. 2*A*). Media from the transfected cells contained low levels of soluble HA-reactive 6- and 25-kDa proteins corresponding to mature TGF-α and larger fully glycosylated forms cleaved only at the C-terminal site (48). High speed centrifugation of conditioned media confirmed that the 25-kDa protein was soluble and not membrane-associated (data not shown). In some experiments, the species appeared as closely spaced doublets. Inclusion of the metalloprotease inhibitor, TAPI-2, in the culture increased levels of the precursor forms (Fig. 2*A*), decreased the 16-kDa tail, and shifted media forms to higher molecular weight, implicating metalloproteases in residual pro-TGF-α processing in EC-2 cells. As observed previously (31), cotransfection of TACE decreased the 36-kDa proform, dramatically increased levels of the 16-kDa, FLAG-reactive residual cytoplasmic tail (Fig. 2*A*), and increased levels of both the soluble 6- and 25-kDa growth factors. An ELISA confirmed the large (~17-fold) TAPI-inhibitable increase in media TGF-α seen in Fig. 2*A* when cells were cotransfected with TGF-α and TACE as compared with cells transfected with TGF-α alone (data not shown).

Transfection of the pro-BTC cDNA into EC-2 fibroblasts produced several forms of cell-associated BTC, including prominent species of ~36 and 42 kDa that were recognized by anti-HA (Fig. 2*A*) and anti-FLAG (data not shown). These likely correspond to variably glycosylated full-length forms, because murine BTC has three *N*-glycosylation sites (49). An 18-kDa protein recognized only by anti-FLAG (Fig. 2*A*) likely corresponds to the residual TM/cytoplasmic domains (50). Media contained several HA-reactive species ranging from 32 to 36 kDa, close to the size reported for purified mouse BTC (49). TAPI-2 treatment led to accumulation of the larger BTC forms in cell lysate and diminished the levels of 18-kDa tail as well as the soluble media proteins (Fig. 2*A*). In contrast to results with pro-TGF-α, cotransfection of TACE did not affect the relative levels of the variously sized BTC proteins present in EC-2 lysates or media, although it did produce a minor new species of ~20 kDa (Fig. 2*A*), which may correspond to a previously identified N-terminal cleavage product observed in transfected CHO and MCF-7 cells (50).

Transfection of the pro-EPR cDNA alone produced cell-associated proteins of ~20, 38, and 40 kDa that were recognized by both anti-HA (Fig. 2*A*, *lane 1*, *EPR*) and anti-FLAG (data not shown). Identification of the 20-kDa form (Fig. 2*A*) as an N-terminally processed EPR (42) is consistent with the selective loss of this HA- and FLAG-reactive species in lysates from TAPI-2-treated cells. FLAG, but not HA antibody, additionally recognized a 17-kDa protein presumably corresponding to the residual TM/cytoplasmic domains (Fig. 2*A*). The sizes of the various products are consistent with a previous report (42). Media from EPR-transfected cells contained low levels of an

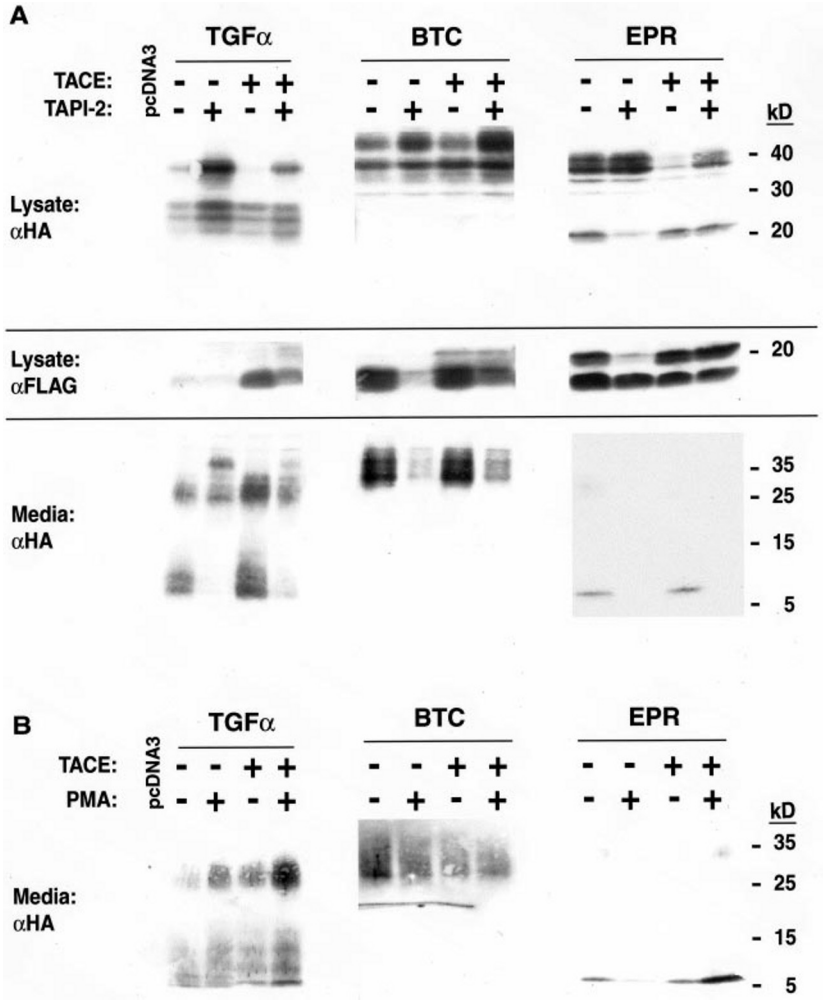

FIG. 2. **Shedding of BTC and EPR is not enhanced by cotransfection of TACE in EC-2 fibroblasts.** EC-2 fibroblasts (43) were transiently transfected with epitope-tagged murine TGF-α, BTC, or EPR cDNAs alone or together with murine TACE cDNA in equal amounts as indicated. *A*, after 24 h, cells were switched into conditioning media containing or lacking TAPI-2 (50 μM). After an additional 24 h, cell lysates and media were harvested for Western blot analysis using the HA and FLAG antibodies. Control samples from cells transfected with pcDNA3 are shown on the *far left*. Approximate molecular weights are indicated. *B*, after 48 h, transfected cells were switched into serum-free media containing or lacking PMA (100 ng/ml). After 2 h, media from three identical plates for each sample were harvested and pooled for Western blot analysis by using the HA antibody.

HA-reactive, ~6-kDa protein that is consistent in size with the purified mouse growth factor (51). TAPI-2 treatment reduced the levels of this soluble protein (Fig. 2*A*). Most important, cotransfection of TACE reduced the levels of intact pro-EPR species but had no effect on levels of the 20- or 17-kDa cell-associated or 6-kDa soluble products (Fig. 2*A*).

Collectively, these results implicate a metalloprotease other than TACE in constitutive C-terminal BTC and EPR cleavage, but leave open the possibility that TACE contributes to the N-terminal processing of the respective precursors.

PMA-induced EPR Shedding Is TACE-dependent—Although TACE did not affect constitutive shedding of BTC or EPR from EC-2 cells, it could have a role in the regulated shedding of these growth factors. To assess this possibility, transfected EC-2 fibroblasts were incubated with 100 ng/ml PMA for 2 h prior to harvesting media and cell lysates. PMA increased media TGF-α levels in cultures cotransfected with TGF-α and TACE as compared with untreated cultures (Fig. 2*B*). In contrast, PMA did not affect the levels of media BTC shed from cells cotransfected with TACE (Fig. 2*B*), which is consistent with a previous report (50) that PMA did not stimulate BTC processing. However, PMA markedly increased the levels of media EPR shed from cells cotransfected with TACE (Fig. 2*B*), indicating that TACE may have a role in PMA-induced shedding of EPR.

TACE Cleaves HB-EGF and AR Ectodomains in Vitro—We confirmed previously that TACE correctly cleaved both the N- and C-terminal processing sites of pro-TGF-α *in vitro* (31). Here we examined the ability of recombinant, soluble TACE to cleave directly the ectodomains of other EGF family precursors. As with pro-TGF-ecto (31), the constructs used encoded ectodomains truncated immediately prior to the transmembrane domain (Fig. 1*B*). HA epitopes were incorporated into the mature growth factor sequences as with the full-length precursors (31, 41), whereas FLAG epitopes were incorporated at the new C termini. These constructs were transiently transfected into COS-1 cells, and the soluble ectodomains were harvested from conditioned media as described under "Experimental Procedures." Correct folding of the mature EGF-like sequence was confirmed for each ectodomain by demonstrating that conditioned media activated EGFR in a dose-dependent fashion when added to receptor-positive cells (52) (data not shown).

To assess cleavage *in vitro*, ectodomains were incubated in buffer or buffer containing TACE at concentrations of either 150 (AR, HB-EGF) or 300 μg/ml (BTC, EPR) from 0 to 24 h at 37 °C. Products were then resolved by SDS-PAGE and probed with anti-HA or anti-FLAG (Fig. 3). In the absence of TACE, pro-ARecto migrated as a heterogeneous 31-kDa species. Addition of TACE rapidly converted this otherwise stable protein to persistent species of 17–20 kDa that were recognized by both anti-HA and anti-FLAG and therefore corresponded to N-terminal cleavage products (Fig. 3). In contrast, a novel species of ~12 kDa accumulated more slowly and was recognized only by anti-HA; this product likely corresponded to a C-terminal cleavage event (Fig. 3). These results suggest that TACE is capable of cleaving both N- and C-terminal sites in the pro-AR ectodomain.

To identify the critical site of C-terminal cleavage, we incubated the reaction products with anti-FLAG beads to capture the short C-terminal product generated by TACE cleavage (not

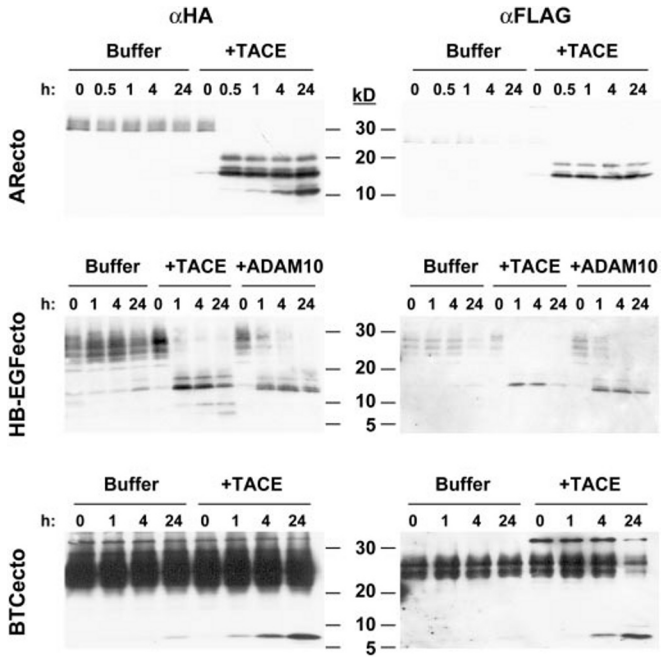

FIG. 3. **Cleavage of EGF ligand ectodomains.** Ectodomains were prepared as described under "Experimental Procedures" and incubated in the presence and absence of recombinant human TACE (150 μg/ml: AR, HB-EGF; 300 μg/ml: BTC, EPR) for 0–24 h. pro-HB-EGFecto was also incubated with recombinant human ADAM10 (150 μg/ml) for 0–24 h. Reactions were stopped by the addition of SDS-PAGE sample buffer and analyzed by Western blot analysis using the HA and FLAG antibodies.

visible by SDS-PAGE) (31, 33, 46). A unique TACE-dependent peak of *m/z* 2453.3 was identified, and the isotopic expansion of this peak confirmed its peptide origin (Fig. 4*B*, *inset*). This peak represented cleavage of pro-AR at ^{176}EKSMK ↓ THSED^{185} (Fig. 4*A*), which is three amino acids downstream from the C terminus of the human protein purified from TPA-stimulated cells (K ↓ S) (53). MALDI-TOF/MS analysis of the larger products present in the digests yielded modest, but reproducible, peaks of *m/z* 12,963 and 14,872 (data not shown), which respectively represented the N-terminal cleavage at ^{78}EEYDN ↓ EPQIS^{87} and ^{95}VRVEQ ↓ VIKPK^{104} and could have produced the 20- and 17-kDa products observed in Fig. 3. Two alternative human N-terminal cleavage sites have been identified, ^{96}YIVDD ↓ SVRVE^{105} and ^{102}VRVEQ ↓ VVKPP^{111} (53). Thus, the TACE-dependent ^{99}Q ↓ V^{100} cleavage product matched the shorter human AR form.

Heterogeneous pro-HB-EGFecto species were observed in the absence of TACE, with predominant forms ranging from 25 to 30 kDa. TACE rapidly converted the larger ectodomain species to two products of 16 and 17 kDa that were recognized by both anti-HA and anti-FLAG (Fig. 3), and thus derived from N-terminal cleavage. Although low levels of the ~16-kDa product were present prior to incubation, they increased only slightly in the absence of added enzyme. Additionally, products of 8 and 9 kDa accumulated in the presence of TACE, were recognized only by anti-HA, and thus judged to be C-terminal cleavage products (Fig. 3).

Direct MALDI/TOF analysis of 24-h HB-EGF digestion products bound to anti-FLAG beads revealed a TACE-dependent product of *m/z* 2570.1, representing cleavage at ^{145}GLTLP ↓ VENPL^{154} (Fig. 4) and matching precisely the C terminus of the purified human protein (54). Thus, the 8- and 9-kDa products observed on SDS-PAGE (Fig. 3) likely had the same C terminus but different N termini (corresponding to the 16- and 17-kDa products). Direct MALDI-TOF/MS analysis of the 1-h digestion products identified a TACE-dependent product of *m/z* 16,209 (data not shown), corresponding to N-terminal cleavage at ^{29}LRRGL ↓ AAATS^{38}. Cleavage at this site would be expected to generate an N-terminal HA- and FLAG-reactive protein of ~16 kDa. The N terminus of mouse HB-EGF has not been identified, but the human protein has multiple N termini (^{31}R ↓ G^{32}; ^{62}R ↓ D^{63}; ^{72}L ↓ R^{73}; ^{73}R ↓ V^{74}) (55–58). The TACE cleavage site identified here occurs 2 amino acids C-terminal of the ^{31}R ↓ G^{32} site.

Because ADAM9 (38) and -10 have been implicated as pro-HB-EGF convertases (23, 39), we tested their ability to cleave pro-HB-EGFecto *in vitro*. ADAM9, at a concentration of 150 μg/ml, did not cleave pro-HB-EGFecto (data not shown). ADAM10 converted pro-HB-EGFecto to HA- and FLAG-reactive 15- and 16.4-kDa N-terminal cleavage products, slightly smaller than those observed with TACE (Fig. 3). No HA-only reactive products corresponding to C-terminal cleavage were observed. Despite lack of a detectable band on SDS-PAGE, we analyzed 24-h total digestion products bound to anti-FLAG beads by MALDI-TOF/MS and identified a single ADAM10 C-terminal cleavage site at ^{151}ENPLY ↓ TYDHT^{160} (data not shown); this site is downstream from the C terminus of human HB-EGF and, by comparison to the cleavage sites of other EGF family precursors, likely is too close to the membrane to represent a physiologic cleavage site. Direct analysis of 1-h digestion products identified a single ADAM10 N-terminal cleavage site of ^{85}TPSKE ↓ RNGKK^{94} as well (data not shown), which did not correspond to any of the known N termini of the human protein.

In the absence of TACE, heterogeneous BTCecto species of ~26 kDa were observed (Fig. 3). Low levels of a 9-kDa species accumulated when incubated with a concentration of TACE twice that used for AR or HB-EGF (300 *versus* 150 μg/ml; no products were observed with the lower concentration). The 9-kDa species was recognized by both anti-HA and anti-FLAG and hence derived from N-terminal cleavage (Fig. 3). No HA-only reactive products indicative of C-terminal cleavage were observed. Similarly, heterogeneous higher molecular weight pro-EPRecto species were converted to an HA/FLAG-reactive ~9-kDa product in the presence of 300 μg/ml TACE (data not shown), and no C-terminal cleavage products were observed. Because of the low levels of the ~9-kDa BTC and EPR products, we were unable to identify the corresponding N-terminal cleavage sites by MALDI-TOF/MS (Fig. 4 and data not shown).

TACE-dependent Cleavage Is Determined by the Juxtamembrane Domain—Our results indicate that TACE is not an efficient C-terminal convertase for pro-BTC or pro-EPR either in cell culture or *in vitro*. To gain insights into the primary sequence features that determine which EGF family precursors are efficient TACE substrates, we aligned the juxtamembrane domains of the EGF ligands. In addition to sequence differences at the scissile bond, the juxtamembrane stalks of pro-BTC and pro-EPR are shorter when compared with pro-TGF-α (14 and 15 amino acids, respectively *versus* 16 amino acids) (Fig. 5).

To assess whether these differences in sequence and stalk length affect TACE cleavage, we created a series of pro-TGF-α mutants differing with respect to stalk features, and we compared their processing to wild-type TGF-α in transfected TACE-positive (25) CHO cells. As shown in Fig. 6*A*, the native stalk of pro-TGF-α was replaced with the counterpart sequence from BTC in TGF-JMBTC. For TGF-JMΔ2, the two terminal amino acids were truncated from the pro-TGF-α stalk to model the BTC stalk length. For TGF-JM$_{\text{LAVV-FYLQ}}$, the P2–P2′ cleavage site amino acids of TGF-α (LAVV) were replaced with those of BTC (FYLQ) (Fig. 6*A*). Fig. 6*B* confirms that these epitope-

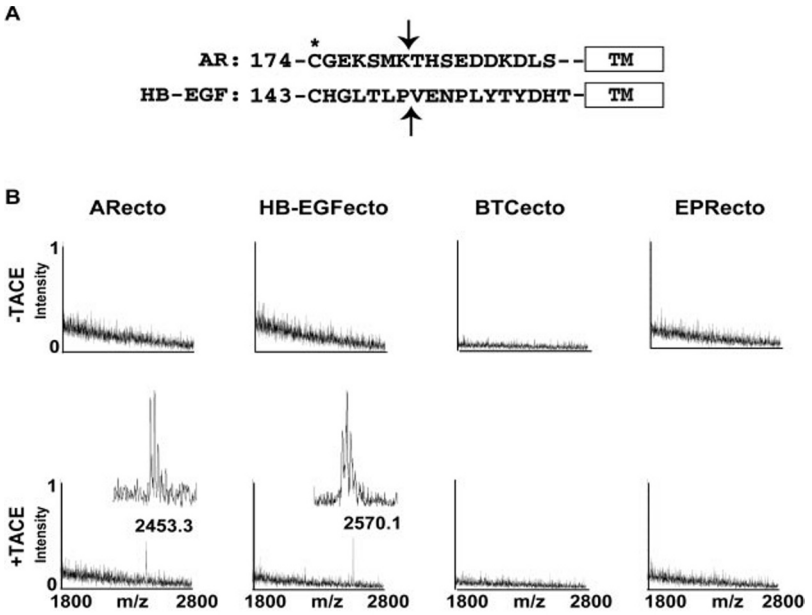

FIG. 4. **MALDI-TOF/MS determination of TACE C-terminal cleavage sites.** *A,* the juxtamembrane stalks of mouse pro-ARecto and pro-HB-EGFecto. The last cysteine of the EGF-like domain is indicated by an *asterisk*, and the location of the TM domain is indicated by the *box. Arrows* denote the TACE cleavage sites, numbered according to the preproprotein, beginning with the methionine of the signal peptide. *B,* C-terminal cleavage products determined by MALDI-TOF/MS. Samples shown were incubated in the absence or presence of recombinant human TACE for 24 h as shown in Fig. 3. Reactions were stopped by the addition of 10 μM EDTA to cleavage products bound to FLAG-affinity resin (Sigma) and spotted directly onto the MALDI target. Spectra above are from samples incubated without TACE, those below in the presence of TACE. *Insets* show the isotopic expansion of the indicated product peak.

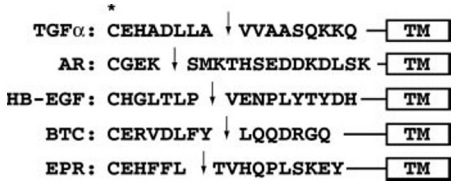

FIG. 5. **Alignment of the EGF ligand juxtamembrane domains.** Sequences of the juxtamembrane stalks aligned beginning with the last cysteine of the EGF-like domain (*). The termini identified in the purified, soluble mouse (TGF-α, BTC, EPR) or human (AR, HB-EGF) proteins are indicated with *arrows.* The TM domain is indicated.

tagged mutant proteins were comparably expressed in CHO cells. Additionally biotinylation experiments confirmed cell surface expression in each case (data not shown).

A TGF-α-specific ELISA revealed that shedding of TGF-α proteins was reduced to near background levels when cells expressed either of the truncated mutants, TGF-JMBTC or TGF-JMΔ2 (Fig. 6*C*, adjusted exact p values = 0.007). Shedding was also drastically decreased in the case of TGF-$JM_{LAVV\text{-}FYLQ}$, although in other experiments shedding was reduced only 2-fold by this substitution of the BTC P2–P2′ recognition site (data not shown).

To confirm the roles of these sequences, we created the corresponding epitope-tagged pro-BTC mutants (Fig. 7*A*), and we observed analogous results. We confirmed expression and cell surface biotinylation of each protein (data not shown), but we analyzed these mutant proteins by an HA/BTC sandwich ELISA. Most interesting, CHO cells did not shed substantial levels of transfected WT-BTC (Fig. 7*B*), but media BTC was readily detected when CHO cells expressed the BTC mutant containing the TGF-α juxtamembrane stalk (BTC-JMTGF) (Fig. 7*B*, adjusted exact p values = 0.009). Although lengthening the BTC stalk by two residues (BTC-JM+2) had only a modest effect on shedding and replacement of the P2–P2′ sequence (BTC-$JM_{FYLQ\text{-}LAVV}$) had no discernible effect, combining these changes (BTC-$JM_{FYLQ\text{-}LAVV}$+2) dramatically enhanced shedding (Fig. 7*B*). Collectively, these data indicate that stalk length is a major determinant of efficient TACE-mediated cleavage and that the small apolar residues of the pro-TGF-α cleavage site are preferred. Additionally, the BTC results suggest that stalk conformation may also have an influence on shedding.

DISCUSSION

Identification of the metalloproteases responsible for shedding EGF family growth factors has received considerable attention recently, particularly due to the importance of these enzymes in regulating EGFR signaling, including via GPCR transactivation. We and others (27, 31) have previously identified TACE as a major TGF-α convertase on the basis of genetic, cell biologic, and biochemical evidence. Here we extend previous findings to support identification of TACE as an AR and HB-EGF convertase. In contrast, our findings do not support a role for TACE in the shedding of BTC or in the constitutive release of EPR. However, TACE could have a role in regulated, PMA-inducible EPR shedding. While this paper was being reviewed, Sahin *et al.* (59) described evidence from studies of ADAM9, -12, -15, and TACE knockout cells that supported a role for TACE as a key mediator of both constitutive and PMA-regulated shedding of TGF-α, AR, HB-EGF, and EPR but not BTC or EGF. Thus, our results are in general agreement with their findings but differ with respect to a positive role for TACE in constitutive EPR shedding. Conceivably, this contradiction could be due to differences in cell populations assayed or used by Sahin *et al.* (59) of an AP-EPR chimeric reporter.

The finding that TACE cleaved the C-terminal juxtamembrane stalk of pro-ARecto *in vitro* (Fig. 3) extends our previous report (31) that cotransfection of TACE promoted AR shedding from EC-2 cells and is consistent with results from several laboratories, including a recent report (59) demonstrating reduced AR shedding from primary $TACE^{\Delta Zn/\Delta Zn}$ fibroblasts. For example, antisense oligonucleotides to TACE but not ADAM9 or -10 blocked AR shedding and EGFR transactivation triggered by smoke-induced oxygen free radicals (36). Inhibition of TACE by RNA interference or expression of a dominant/negative enzyme also suppressed GPCR-stimulated AR release and EGFR signaling in squamous carcinoma cells (24). Recently, we found that mammary gland rudiments from TACE-deficient fetuses display impaired ductal outgrowth when transplanted into nude mice.[2] A similar defect was observed upon transplantation of EGFR null mammary rudiments (60), and ductal development was stunted in pubescent female mice lacking AR

[2] M. D. Sternlicht, S. W. Sunnarborg, D. C. Lee, and Z. Werb, unpublished observations.

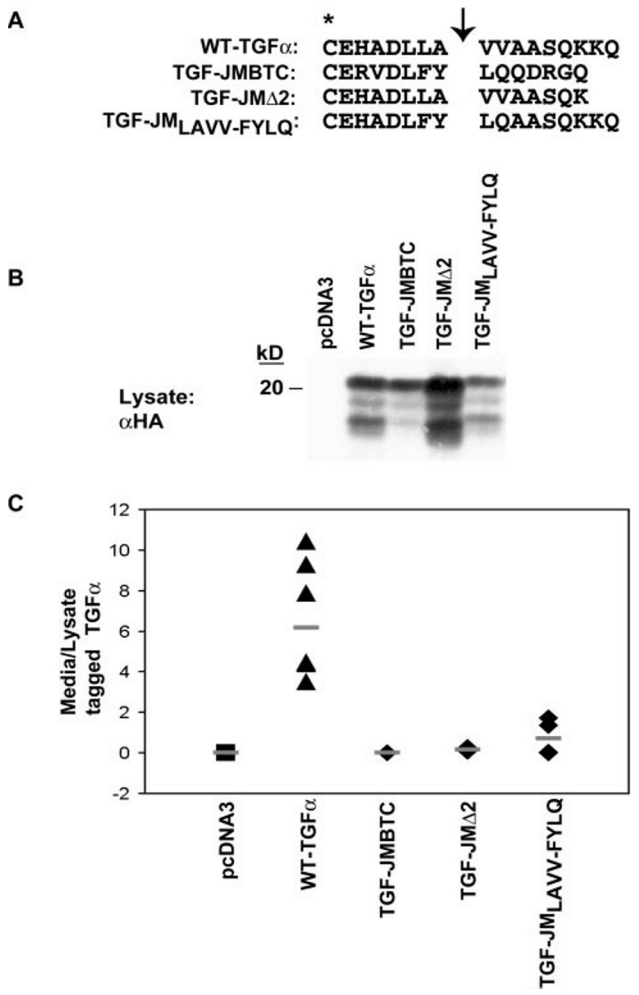

FIG. 6. **TGF-α juxtamembrane stalk mutations.** *A*, TGF-α juxtamembrane stalk mutants. The terminal cysteine of the EGF-like domain is indicated (*), and the C-terminal cleavage site of wild-type (*WT*) pro-TGF-α (*WT-TGF-α*) is indicated by an *arrow*. *B*, expression of juxtamembrane domain mutants in CHO cells. CHO cells were transiently transfected with pcDNA3 vector or juxtamembrane domain mutants, and 24 h later, cells were switched to conditioning media. After an additional 24 h, lysates were harvested for Western blot analysis using the HA antibody. Note that CHO cells have been shown previously to express different molecular weight forms of TGF-α (80) compared with EC-2 cells (31). *C*, shedding of TGF-α juxtamembrane stalk mutants is impaired. CHO cells were transiently transfected with pcDNA3 vector or the juxtamembrane domain mutants. Twenty-four hours following transfection, cells were switched to conditioning media. After an additional 24 h, media and lysates were harvested and analyzed by sandwich ELISA by using the HA and TGF-α antibodies. Results are expressed as the ratio of media to lysate TGF-α and represent two separate experiments analyzed in triplicate. The *gray line* represents the median.

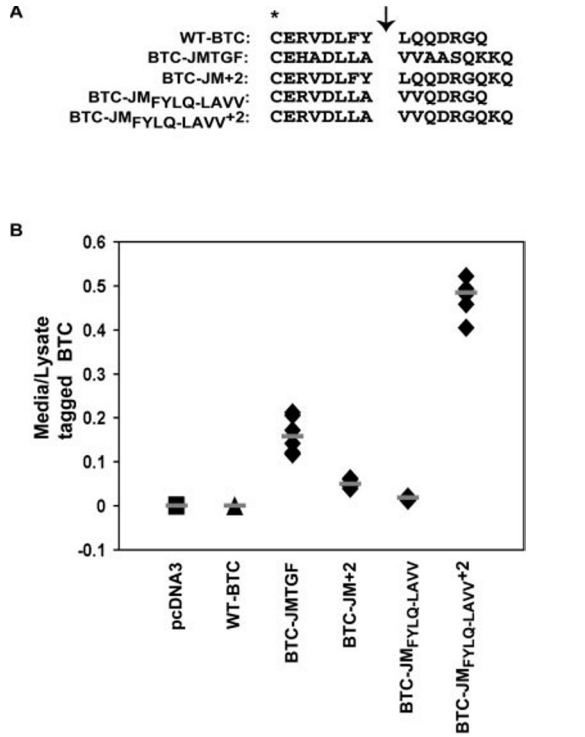

FIG. 7. **BTC juxtamembrane stalk mutations.** *A,* BTC juxtamembrane domain mutants. The terminal cysteine of the EGF-like domain is indicated (*), and the C terminus of purified, soluble mouse BTC is indicated by an *arrow*. *B,* sandwich ELISA of conditioned media and lysates. CHO cells were transiently transfected with wild-type (*WT*) or mutant proteins, and 24 h later, cells were switched to conditioning media. After an additional 24 h, media and lysates were harvested and analyzed by sandwich ELISA by using the HA and BTC antibodies. Results are presented as the ratio of media to lysate-tagged BTC and represent two separate experiments analyzed in triplicate. The *gray line* represents the median.

(12). Thus, the present findings add to a growing body of evidence implicating TACE as a major mediator of AR-induced biological responses.

On the other hand, the C-terminal site cleaved by TACE *in vitro* (Fig. 4) did not match the C terminus of the soluble human AR protein ($^{183}E \downarrow K^{184}$) purified from TPA-treated MCF-7 cell media by Shoyab *et al.* (61), which was only three amino acids downstream from the terminal Cys of the EGF-like motif. However, it has been suggested by others that this is not the *bona fide* C terminus of naturally secreted AR protein, because this form is much less potent with respect to EGFR activation and mitogenicity compared with recombinant AR proteins containing C-terminal extensions (62, 63). In particular, a recombinant AR containing three additional amino acids, which corresponds precisely to the form predicted from the *in vitro* TACE cleavage site, possessed >40-fold higher EGFR binding and mitogenic activities compared with the truncated $^{183}E \downarrow K^{184}$ protein, and it corresponded closely to the respective activities of MCF-7 conditioned media (62). A soluble AR species, inconsistent in size with a C terminus of $^{183}E \downarrow K^{184}$, was released from Madin-Darby canine kidney cells, suggesting that AR is cleaved more distally to the EGF-like domain (64). Moreover, the $^{183}E \downarrow K^{184}$ position places cleavage closer to the EGF-like motif and further from the cell membrane than is observed with other EGF family ligands (Fig. 5). Thus, we propose that the site cleaved by TACE *in vitro* (mouse $^{180}K \downarrow T^{181}$; equivalent to human $^{187}K \downarrow T^{188}$) is physiologically relevant.

HB-EGF shedding has been the focus of considerable attention, due in part to its role in GPCR-induced EGFR transactivation as well as interest in the potential juxtacrine roles of pro-HB-EGF. However, the identity of the HB-EGF convertase has been controversial. Our previous findings indicate that TACE is an important physiologic regulator of HB-EGF shedding. HB-EGF knockout and TACE-deficient mice displayed indistinguishable cardiac valve and lung development defects (14, 35), and cotransfected TACE promoted shedding of HB-EGF from TACE-deficient cells (31). Moreover, HB-EGF shedding from primary fibroblasts was impaired in TACE-deficient cells (59). Here we additionally show that TACE cleaved pro-HB-EGFecto *in vitro* at a site in the juxtamembrane domain (Figs. 3 and 4) corresponding to the C terminus of the HB-EGF protein purified from TPA-stimulated Vero-H cells (54).

Other metalloproteases, including ADAM9, -10, and -12, have also been proposed as candidate HB-EGF convertases.

Dominant negative ADAM9 (MDC9/meltrin-γ) inhibited stimulus-induced shedding of HB-EGF in Vero-H cells (38), although ADAM9-null mice did not display an overt phenotype, and cells derived from them shed HB-EGF normally (65). Additionally, a dominant negative ADAM9 did not interfere with HB-EGF cleavage-dependent GPCR transactivation of EGFR (19), and as described here, ADAM9 did not cleave pro-HB-EGFecto *in vitro* (data not shown). Dominant negative ADAM10 and/or antisense oligonucleotides blocked GPCR-induced HB-EGF shedding and EGFR transactivation, respectively, in COS7 (23) and mucosal epithelial cells (39). However, whereas ADAM10 cleaved the juxtamembrane stalk of pro-HB-EGFecto in our studies (Fig. 3), the cleavage site was located several residues downstream of the C terminus of mature HB-EGF, closer to the transmembrane domain than is observed with other EGF family precursors. Because ADAM10 knockout mice died at embryonic day 9.5 exhibiting multiple defects, including severely delayed heart development (66), a direct comparison to the later and more restricted valvulogenesis defects displayed by HB-EGF knockouts is not possible. ADAM12 has been linked to the role of HB-EGF in experimentally induced cardiac hypertrophy. A dominant negative ADAM12 blocked GPCR-induced HB-EGF shedding from cardiomyocytes, and a novel metalloprotease inhibitor of HB-EGF shedding bound ADAM12 and also attenuated both HB-EGF shedding and hypertrophic changes in a mouse model (21). Like HB-EGF null mice, a significant proportion of mice lacking ADAM12 die prior to weaning, and fibroblasts from ADAM12-null mice did not shed HB-EGF in response to TPA (67). However, cardiac defects were not observed in this model. ADAM19 knockout mice displayed enlarged cardiac valves, replicating at least part of the HB-EGF-deficient phenotype (68). On the other hand, cell-based studies using primary fibroblasts from ADAM19, -10, and -9/12/15 knockout mice indicated that HB-EGF shedding is not impaired in these cells. Moreover, a batimastat-insensitive activity was also implicated in shedding (59). Finally, MMP-3 (69) and MMP7/matrilysin (70) have also been put forth as candidate HB-EGF convertases. Conceivably, multiple proteases could contribute to HB-EGF shedding in a cell type- and stimulus-dependent manner.

In contrast to its actions on the HB-EGF and AR precursors (31), TACE did not enhance the constitutive ectodomain shedding of either BTC or EPR from cotransfected EC-2 cells, and it did not efficiently cleave the juxtamembrane stalks of either ectodomain *in vitro*. Constitutive shedding of BTC and EPR were metalloprotease-dependent, as TAPI-2 blocked production of the soluble media forms (Fig. 2*A*). However, TACE may have a role in PMA-stimulated EPR shedding (Fig. 2*B*). Most interesting, CHO cells that normally express TACE (25) did not efficiently release BTC and instead accumulated membrane-associated forms (Fig. 7*B*). Our results also confirm the report from a recent study that secretion of a transfected BTC/alkaline phosphatase fusion protein was not stimulated by phorbol esters (50), an observation that distinguishes BTC processing from that of other EGF family members, including EPR (42). These observations raise the possibility that pro-BTC is acted upon by another metalloprotease or instead functions predominantly through juxtacrine actions involving membrane-associated forms. Unlike TACE-deficient mice, BTC knockout mice did not display an overt phenotype (14). Identifying the metalloprotease(s) responsible for C-terminal cleavage of BTC, EPR, and EGF will be key to understanding the biology of these growth factors. Recently, Sahin *et al.* (59) identified ADAM10 as a BTC sheddase, although we were unable to confirm ADAM10 cleavage of BTCecto *in vitro* (data not shown).

Evidence that TACE is a major C-terminal convertase for some EGF family members (*e.g.* TGF-α, AR, and HB-EGF) but not others (BTC and EPR) raises the question as to what structural features are recognized by sheddases. Because the sequence and length of juxtamembrane stalks of EGF family precursors (Fig. 5) are not conserved, sheddase action must be specified by other structural features. For example, substitution of stalk sequences from normally shed proteins for those of integral membrane proteins not subject to shedding conferred constitutive shedding in the latter (71, 72). Moreover, the length of the stalk may be an important determinant, because mutagenesis of the TNF precursor (73) or the growth hormone receptor (74) revealed a minimum stalk length for efficient processing, presumably reflecting accessibility of the cleavage site to the relevant metalloprotease. The distance from the cleavage site to the membrane may be an important determinant of cleavage. Studies of Kit ligand processing in which the stalk sequence was reiterated revealed that cleavage occurred only at the most membrane proximal cleavage site (75), consistent with a mechanism specified by distance from the membrane. In contrast, studies of angiotensin-converting enzyme/CD4 (76) or L-selectin/B7.2 (72) chimeric proteins underscored the importance of the distal ectodomain as a primary determinant of efficient shedding. Moreover, although they share the same stalk, the testis angiotensin-converting enzyme isoform was shed more efficiently (77), presumably due to the presence of a distal structural motif that was recognized by the processing enzyme (78).

Undoubtedly, the sequence of the cleavage site must impact shedding efficiency as well. A study of macrophage colony-stimulating factor shedding indicated that both the scissile bond sequence and the distance from the membrane determined cleavage (79). The fact that TACE cleaves TNF $>$ TGF-α $>$ AR/HB-EGF suggests it prefers small apolar amino acids in the P1 and P1′ positions (31). Our present results are in keeping with these indications, because lengthening the pro-BTC stalk either directly or by substituting the pro-TGF-α stalk stimulated BTC shedding, whereas the converse manipulations to pro-TGF-α reduced TGF-α shedding. The effect of lengthening the pro-BTC stalk was enhanced by simultaneously substituting the preferred P2–P2′ recognition site of pro-TGF-α. Thus, the combination of stalk length and scissile bond sequence determines the efficiency of EGF family shedding.

In addition to cleaving the juxtamembrane stalks of pro-TGF-α, pro-AR, and pro-HB-EGF, TACE also cleaved these precursors at one or more N-terminal sites. In the case of pro-TGF-α, we previously established that TACE correctly cleaved the physiologic N-terminal processing site *in vitro* (31). Here, we showed that TACE cleaved mouse pro-ARecto *in vitro* at a site ($^{99}Q \downarrow V^{100}$) corresponding to one of two N termini identified for human AR purified from cell culture (53). Human HB-EGF purified from cell culture also displayed heterogeneous N termini corresponding to $^{31}R \downarrow G^{32}$, $^{62}R \downarrow D^{63}$, $^{72}L \downarrow R^{73}$, and $^{73}R \downarrow V^{74}$ (55–58). TACE cleaved mouse HB-EGF *in vitro* two residues downstream of $^{31}R \downarrow G^{32}$ to produce a protein that retained the heparin binding domain. Whether this corresponds to a *bona fide* N terminus of the murine protein is presently unclear. TACE also cleaved the N-terminal regions of pro-BTC and pro-EPR (Figs. 2 and 3), albeit less efficiently, thus precluding identification of the cleavage sites. Most interesting, TACE invariably cleaved the N-terminal regions of EGF family precursors more rapidly and with greater efficiency than it cleaved the stalk regions. This observation agrees with an earlier cell-based study that revealed more rapid processing of the pro-TGF-α N-terminal site compared with the stalk cleavage site (80).

The possibility that TACE mediates both N- and C-terminal

cleavage events in the EGF family raises the interesting question as to how this membrane-anchored protease cleaves distant sites separated by the EGF-like motif and, in some cases, additional sequences. Identifying the mechanism and recognition elements required for TACE-dependent N-terminal cleavage events may provide more insight into the requirements and relative inefficiency of C-terminal cleavage.

Acknowledgments—We thank David Threadgill (University of North Carolina, Chapel Hill) for providing the mouse epiregulin cDNA and Roy Black (Amgen Inc., Seattle, WA) for providing recombinant human TACE. We also thank Brenda Temple (University of North Carolina, Chapel Hill) for assistance with sequence alignment and designing juxtamembrane stalk mutants, Dominic Moore for statistical analysis, and Tim Myers and Julie Clarke for critical review of the manuscript.

REFERENCES

1. Lee, D. C., Hinkle, C. L., Jackson, L. F., Li, S., and Sunnarborg, S. W. (2003) in *The Cytokine Handbook* (Thomson, A. W., and Lotze, M. T., ed) 4th Ed., pp. 959–987, Elsevier Science Ltd., London
2. Brachmann, R., Lindquist, P. B., Nagashima, M., Kohr, W., Lipari, T., Napier, M., and Derynck, R. (1989) *Cell* **56,** 691–700
3. Wong, S. T., Winchell, L. F., McCune, B. K., Earp, H. S., Teixido, J., Massague, J., Herman, B., and Lee, D. C. (1989) *Cell* **56,** 495–506
4. Takemura, T., Kondo, S., Homma, T., Sakai, M., and Harris, R. C. (1997) *J. Biol. Chem.* **272,** 31036–31042
5. Dong, J., Opresko, L. K., Dempsey, P. J., Lauffenburger, D. A., Coffey, R. J., and Wiley, H. S. (1999) *Proc. Natl. Acad. Sci. U. S. A.* **96,** 6235–6240
6. Iwamoto, R., Handa, K., and Mekada, E. (1999) *J. Biol. Chem.* **274,** 25906–25912
7. Pan, B., Sengoku, K., Goishi, K., Takuma, N., Yamashita, T., Wada, K., and Ishikawa, M. (2002) *Mol. Hum. Reprod.* **8,** 734–741
8. Takemura, T., Hino, S., Okada, M., Murata, Y., Yanagida, H., Ikeda, M., Yoshioka, K., and Harris, R. C. (2002) *Kidney Int.* **61,** 1968–1979
9. Singh, A. B., Tsukada, T., Zent, R., and Harris, R. C. (2004) *J. Cell Sci.* **117,** 1365–1379
10. Luetteke, N. C., Qiu, T. H., Peiffer, R. L., Oliver, P., Smithies, O., and Lee, D. C. (1993) *Cell* **73,** 263–278
11. Mann, G. B., Fowler, K. J., Gabriel, A., Nice, E. C., Williams, R. L., and Dunn, A. R. (1993) *Cell* **73,** 249–261
12. Luetteke, N. C., Qiu, T. H., Fenton, S. E., Troyer, K. L., Riedel, R. F., Chang, A., and Lee, D. C. (1999) *Development* **126,** 2739–2750
13. Iwamoto, R., Yamazaki, S., Asakura, M., Takashima, S., Hasuwa, H., Miyado, K., Adachi, S., Kitakaze, M., Hashimoto, K., Raab, G., Nanba, D., Higashiyama, S., Hori, M., Klagsbrun, M., and Mekada, E. (2003) *Proc. Natl. Acad. Sci. U. S. A.* **100,** 3221–3226
14. Jackson, L. F., Qiu, T. H., Sunnarborg, S. W., Chang, A., Zhang, C., Patterson, C., and Lee, D. C. (2003) *EMBO J.* **22,** 2704–2716
15. Marikovsky, M., Breuing, K., Liu, P. Y., Eriksson, E., Higashiyama, S., Farber, P., Abraham, J., and Klagsbrun, M. (1993) *Proc. Natl. Acad. Sci. U. S. A.* **90,** 3889–3893
16. Takemura, T., Hino, S., Kuwajima, H., Yanagida, H., Okada, M., Nagata, M., Sasaki, S., Barasch, J., Harris, R. C., and Yoshioka, K. (2001) *J. Am. Soc. Nephrol.* **12,** 964–972
17. Nelson, K. G., Takahashi, T., Lee, D. C., Luetteke, N. C., Bossert, N. L., Ross, K., Eitzman, B. E., and McLachlan, J. A. (1992) *Endocrinology* **131,** 1657–1664
18. Buteau, J., Foisy, S., Joly, E., and Prentki, M. (2003) *Diabetes* **52,** 124–132
19. Prenzel, N., Zwick, E., Daub, H., Leserer, M., Abraham, R., Wallasch, C., and Ullrich, A. (1999) *Nature* **402,** 884–888
20. Pierce, K. L., Tohgo, A., Ahn, S., Field, M. E., Luttrell, L. M., and Lefkowitz, R. J. (2001) *J. Biol. Chem.* **276,** 23155–23160
21. Asakura, M., Kitakaze, M., Takashima, S., Liao, Y., Ishikura, F., Yoshinaka, T., Ohmoto, H., Node, K., Yoshino, K., Ishiguro, H., Asanuma, H., Sanada, S., Matsumura, Y., Takeda, H., Beppu, S., Tada, M., Hori, M., and Higashiyama, S. (2002) *Nat. Med.* **8,** 35–40
22. McCole, D. F., Keely, S. J., Coffey, R. J., and Barrett, K. E. (2002) *J. Biol. Chem.* **277,** 42603–42612
23. Yan, Y., Shirakabe, K., and Werb, Z. (2002) *J. Cell Biol.* **158,** 221–226
24. Gschwind, A., Hart, S., Fischer, O. M., and Ullrich, A. (2003) *EMBO J.* **22,** 2411–2421
25. Black, R. A., Rauch, C. T., Kozlosky, C. J., Peschon, J. J., Slack, J. L., Wolfson, M. F., Castner, B. J., Stocking, K. L., Reddy, P., Srinivasan, S., Nelson, N., Bolani, N., Schooley, K. A., Gerhart, M., Davis, R., Fitzner, J. N., Johnson, R. S., Paxton, R. J., March, C. J., and Cerretti, D. P. (1997) *Nature* **385,** 729–733
26. Moss, M. L., Jin, S.-L. C., Milla, M. E., Burkhart, W., Carter, H. L., Chen, W.-J., Clay, W. C., Didsbury, J. R., Hassler, D., Hoffman, C. R., Kost, T. A., Lambert, M. H., Leesnitzer, M. A., McCauley, P., McGeehan, G., Mitchell, J., Moyer, M., Pahel, G., Rocque, W., Overton, L. K., Schoenen, F., Seaton, T., Su, J.-L., Warner, J., Willard, D., and Becherer, J. D. (1997) *Nature* **385,** 733–736
27. Peschon, J. J., Slack, J. L., Reddy, P., Stocking, K. L., Sunnarborg, S. W., Lee, D. C., Russell, W. E., Castner, B. J., Johnson, R. S., Fitzner, J. N., Boyce, R. W., Nelson, N., Kozlosky, C. J., Wolfson, M. F., Rauch, C. T., Cerretti, D. P., Paxton, R. J., March, C. J., and Black, R. A. (1998) *Science* **282,** 1281–1284
28. Threadgill, D. W., Dlugosz, A. A., Hansen, L. A., Tennenbaum, T., Lichti, U., Yee, D., LaMantia, C., Mourton, T., Herrup, K., Harris, R. C., Barnard, J. A., Yuspa, S. H., Coffey, R. J., and Magnuson, T. (1995) *Science* **269,** 230–234
29. Sibilia, M., and Wagner, E. F. (1995) *Science* **269,** 234–238
30. Miettinen, P. J., Berger, J. E., Meneses, J., Phung, Y., Pedersen, R. A., Werb, Z., and Derynck, R. (1995) *Nature* **376,** 337–341
31. Sunnarborg, S. W., Hinkle, C. L., Stevenson, M., Russell, W. E., Raska, C. S., Peschon, J. J., Castner, B. J., Gerhart, M. J., Paxton, R. J., Black, R. A., and Lee, D. C. (2002) *J. Biol. Chem.* **277,** 12838–12845
32. Merlos-Suarez, A., Ruiz-Paz, S., Baselga, J., and Arribas, J. (2001) *J. Biol. Chem.* **276,** 48510–48517
33. Hinkle, C. L., Mohan, M. J., Lin, P., Yeung, N., Rasmussen, F., Milla, M. E., and Moss, M. L. (2003) *Biochemistry* **42,** 2127–2136
34. Werb, Z., and Yan, Y. (1998) *Science* **282,** 1279–1280
35. Zhao, J., Chen, H., Peschon, J. J., Shi, W., Zhang, Y., Frank, S. J., and Warburton, D. (2001) *Dev. Biol.* **232,** 204–218
36. Lemjabbar, H., Li, D., Gallup, M., Sidhu, S., Drori, E., and Basbaum, C. (2003) *J. Biol. Chem.* **278,** 26202–26207
37. Le Gall, S., Auger, R., Dreux, C., and Mauduit, P. (2003) *J. Biol. Chem.* **278,** 45255–45268
38. Izumi, Y., Hirata, M., Hasuwa, H., Iwamoto, R., Umata, T., Miyado, K., Tamai, Y., Kurisaki, T., Sehara-Fujisawa, A., Ohno, S., and Mekada, E. (1998) *EMBO J.* **17,** 7260–7272
39. Lemjabbar, H., and Basbaum, C. (2002) *Nat. Med.* **8,** 41–46
40. Mori, S., Tanaka, M., Nanba, D., Nishiwaki, E., Ishiguro, H., Higashiyama, S., and Matsuura, N. (2003) *J. Biol. Chem.* **278,** 46029–46034
41. Briley, G. P., Hissong, M. A., Chiu, M. L., and Lee, D. C. (1997) *Mol. Biol. Cell* **8,** 1619–1631
42. Baba, I., Shirasawa, S., Iwamoto, R., Okumura, K., Tsunoda, T., Nishioka, M., Fukuyama, K., Yamamoto, K., Mekada, E., and Sasazuki, T. (2000) *Cancer Res.* **60,** 6886–6889
43. Reddy, P., Slack, J. L., Davis, R., Cerretti, D. P., Kozlosky, C. J., Blanton, R. A., Shows, D., Peschon, J. J., and Black, R. A. (2000) *J. Biol. Chem.* **275,** 14608–14614
44. Sandgren, E. P., Luetteke, N. C., Palmiter, R. D., Brinster, R. L., and Lee, D. C. (1990) *Cell* **61,** 1121–1135
45. Nemzek, J. A., Siddiqui, J., and Remick, D. G. (2001) *J. Immunol. Methods* **255,** 149–157
46. Raska, C. S., Parker, C. E., Sunnarborg, S., W., Pope, R. M., Lee, D. C., Glish, G. L., and Borchers, C. L. (2003) *J. Am. Soc. Mass Spectrom.* **14,** 1076–1085
47. Papac, D. I., Hoyes, J., and Tomer, K. B. (1994) *Protein Sci.* **3,** 1485–1492
48. Luetteke, N. C., Michalopoulos, G. K., Teixido, J., Gilmore, R., Massague, J., and Lee, D. C. (1988) *Biochemistry* **27,** 6487–6494
49. Shing, Y., Christofori, G., Hanahan, D., Ono, Y., Sasada, R., Igarashi, K., and Folkman, J. (1993) *Science* **259,** 1604–1607
50. Tada, H., Sasada, R., Kawaguchi, Y., Kojima, I., Gullick, W. J., Salomon, D. S., Igarashi, K., Seno, M., and Yamada, H. (1999) *J. Cell. Biochem.* **72,** 423–434
51. Toyoda, H., Komurasaki, T., Uchida, D., Takayama, Y., Isobe, T., Okuyama, T., and Hanada, K. (1995) *J. Biol. Chem.* **270,** 7495–7500
52. Saxon, M. L., and Lee, D. C. (1999) *J. Biol. Chem.* **274,** 28356–28362
53. Shoyab, M., McDonald, V. L., Bradley, J. G., and Todaro, G. J. (1988) *Proc. Natl. Acad. Sci. U. S. A.* **85,** 6528–6532
54. Goishi, K., Higashiyama, S., Klagsbrun, M., Nakano, N., Umata, T., Ishikawa, M., Mekada, E., and Taniguchi, N. (1995) *Mol. Biol. Cell* **6,** 967–980
55. Nakagawa, T., Higashiyama, S., Mitamura, T., Mekada, E., and Taniguchi, N. (1996) *J. Biol. Chem.* **271,** 30858–30863
56. Ono, M., Raab, G., Lau, K., Abraham, J. A., and Klagsbrun, M. (1994) *J. Biol. Chem.* **269,** 31315–31321
57. Higashiyama, S., Lau, K., Besner, G. E., Abraham, J. A., and Klagsbrun, M. (1992) *J. Biol. Chem.* **267,** 6205–6212
58. Higashiyama, S., Abraham, J. A., Miller, J., Fiddes, J. C., and Klagsbrun, M. (1991) *Science* **251,** 936–939
59. Sahin, U., Weskamp, G., Kelly, K., Zhou, H.-M., Higashiyama, S., Peschon, J., Hartmann, D., Saftig, P., and Blobel, C. P. (2004) *J. Cell Biol.* **164,** 769–779
60. Wiesen, J. F., Young, P., Werb, Z., and Cunha, G. R. (1999) *Development* **126,** 335–344
61. Shoyab, M., Plowman, G. D., McDonald, V. L., Bradley, J. G., and Todaro, G. J. (1989) *Science* **243,** 1074–1076
62. Thompson, S. A., Harris, A., Hoang, D., Ferrer, M., and Johnson, G. R. (1996) *J. Biol. Chem.* **271,** 17927–17931
63. Adam, R., Drummond, D. R., Solic, N., Holt, S. J., Sharma, R. P., Chamberlin, S. G., and Davies, D. E. (1995) *Biochim. Biophys. Acta* **1266,** 83–90
64. Brown, C. L., Meise, K. S., Plowman, G. D., Coffey, R. J., and Dempsey, P. J. (1998) *J. Biol. Chem.* **273,** 17258–17268
65. Weskamp, G., Cai, H., Brodie, T. A., Higashyama, S., Manova, K., Ludwig, T., and Blobel, C. P. (2002) *Mol. Cell. Biol.* **22,** 1537–1544
66. Hartmann, D., de Strooper, B., Serneels, L., Craessaerts, K., Herreman, A., Annaert, W., Umans, L., Lubke, T., Lena Illert, A., von Figura, K., and Saftig, P. (2002) *Hum. Mol. Genet.* **11,** 2615–2624
67. Kurisaki, T., Masuda, A., Sudo, K., Sakagami, J., Higashiyama, S., Matsuda, Y., Nagabukuro, A., Tsuji, A., Nabeshima, Y., Asano, M., Iwakura, Y., and Sehara-Fujisawa, A. (2003) *Mol. Cell. Biol.* **23,** 55–61
68. Zhou, H.-M., Weskamp, G., Chesneau, V., Sahin, U., Vortkamp, A., Horiuchi, K., Chiusaroli, R., Hahn, R., Wilkes, D., Fisher, P., Baron, R., Manova, K., Basson, C. T., Hempstead, B., and Blobel, C. P. (2004) *Mol. Cell. Biol.* **24,** 96–104
69. Suzuki, M., Raab, G., Moses, M. A., Fernandez, C. A., and Klagsbrun, M. (1997) *J. Biol. Chem.* **272,** 31730–31737
70. Yu, W. H., Woessner, J. F., Jr., McNeish, J. D., and Stamenkovic, I. (2002) *Genes Dev.* **16,** 307–323
71. Arribas, J., Lopez-Casillas, F., and Massague, J. (1997) *J. Biol. Chem.* **272,** 17160–17165

72. Zhao, L., Shey, M., Farnsworth, M., and Dailey, M. O. (2001) *J. Biol. Chem.* **276,** 30631–30640
73. Tang, P., Hung, M. C., and Klostergaard, J. (1996) *Biochemistry* **35,** 8226–8233
74. Conte, F., Salles, J. P., Raynal, P., Fernandez, L., Molinas, C., Tauber, M., and Bieth, E. (2002) *Biochem. Biophys. Res. Commun.* **290,** 851–857
75. Cheng, H. J., and Flanagan, J. G. (1994) *Mol. Biol. Cell* **5,** 943–953
76. Sadhukhan, R., Santhamma, K. R., Reddy, P., Peschon, J. J., Black, R. A., and Sen, I. (1999) *J. Biol. Chem.* **274,** 10511–10516
77. Woodman, Z. L., Oppong, S. Y., Cook, S., Hooper, N. M., Schwager, S. L., Brandt, W. F., Ehlers, M. R., and Sturrock, E. D. (2000) *Biochem. J.* **347,** 711–718
78. Chubb, A. J., Schwager, S. L., Woodman, Z. L., Ehlers, M. R., and Sturrock, E. D. (2002) *Biochem. Biophys. Res. Commun.* **297,** 1225–1230
79. Deng, P., Wang, Y. L., Haga, Y., and Pattengale, P. K. (1998) *Biochemistry* **37,** 17898–17904
80. Teixido, J., Wong, S. T., Lee, D. C., and Massague, J. (1990) *J. Biol. Chem.* **265,** 6410–6415